INL/CON-07-12173
PREPRINT

Identification of Statistical Invariance for Anodic Signals of Mk-IV Electrorefiner

Global 2007

Supathorn Phongikaroon
Tae-Sic Yoo

September 2007

The INL is a
U.S. Department of Energy
National Laboratory
operated by
Battelle Energy Alliance

Identification of Statistical Invariance for Anodic Signals of Mk-IV Electrorefiner

Supathorn Phongikaroon and Tae-Sic Yoo

Idaho National Laboratory: Materials and Fuels Complex, MS 6180, Idaho Falls, ID 83403,
supathorn.phongikaroon@inl.gov

A statistical invariance technique is proposed for an analysis of anodic signals from the Mk-IV electrorefiner (ER) currently used for treating spent EBR-II fuel. Voltage and applied current signals obtained from the Data Archival Software System (DASS) were used in this study. In general, the plots of these signals from different experimental runs present complex patterns to analyze—the currents were adjusted and shut-off due to limited ampere-hr or cut-off cell voltage; the voltage would increase showing a sign that uranium in the fuel elements had been depleted. Rather than directly analyzing these sets of time-series signals, a simple nonlinear function of these signal sequences and division were observed, which returned resistance series information. The primary idea deriving the methodology presented in this paper is that "anodic resistance time series should show intrinsic kinetic progress of anodic ER process." A simple histogram-based analysis reveals notable statistical information, which may be invariant under ideal ER operating conditions. For instance, the results suggest that mostly uranium dissolution would be preferentially transferred around 0.00217 - 0.00354 ohm and other minor distribution peaks may possibly represent other transfers of fission species in the system.

I. INTRODUCTION

Spent driver fuel from the Experimental Breeder Reactor-II (EBR-II) is currently being treated in the Mk-IV electrorefiner in the Fuel Conditioning Facility (FCF) of Idaho National Laboratory (INL). This important state-of-the-art equipment is the crucial piece of the spent fuel treatment process, because it separates the spent fuel into the following four streams: (1) pure uranium, (2) group actinides (U/TRU), (3) metallic high-level metal waste forms containing the cladding and noble metal fission products, and (4) ceramic high-level waste forms containing sodium and active metal fission products (Refs. 1, 2). In the electrorefining process, current and cell voltage cannot be independently controlled. Their functional dependence on each other depends on cathode type (solid steel or liquid cadmium), temperature, initial fuel composition, mass of oxidants or reductants, and electrorefiner characteristic variables such as initial salt and cadmium pool compositions (Ref. 3).

To understand the electrorefining process, the General Purpose Electrochemical Simulator (GPEC) was developed by Argonne National Laboratory, and modeled the major relevant electrochemical features (Refs. 4, 5). Despite the achievement of its development, the GPEC code does not always result in a solution, and experimental results must often be supplied to provide an empirical solution. The reasons behind these issues are due to (1) many empirically-derived coefficients (e.g. density and viscosity of mixture, surface overpotential, current exchange density, activity coefficients of mixture species, sticking coefficient and dendritic form factor), (2) many regions and interfaces that needed to be solved simultaneously causing error propagation for parameters in mathematical schemes, and (3) restricted geometry inputs. Aside from these functionality issues, the GPEC code has a structure that is difficult to upgrade, its use is not easily learned, and it has an incomplete set of transport couplings (electrochemistry via mass, momentum, and heat transfer). This concern provided the motivation to develop a new mathematical approach to the Mk-IV electrorefiner at INL.

The main objective of this study is to find a statistical invariance from the given operational signals (for example, current and voltage) that would help yield important information or characteristics of the system. The approach focuses on the anodic side of the Mk-IV ER using the primary idea that *anodic resistance time series should show intrinsic kinetic progress of anodic ER process*. A histogram-based analysis technique is proposed and applied to analyze the signals obtained from the Data Archival Software System (DASS).

II. EQUIPMENT, PROCESS AND COMPOSITIONS

The Mark-IV ER and its system are currently operated in an argon hot cell environment locating in the Fuel Conditioning Facility (FCF). The ER cylindrical vessel made of stainless steel with both an inside diameter and a height of 1.0 m. The bottom layer of the vessel contains about 0.1 m of molten cadmium. This layer is covered with about 0.3 m in height of molten LiCl-KCl eutectic salt containing approximately 10 weight percents (wt%) of UCl_3. The operating temperature is typically at 500 °C; however, some experiments were also conducted at 450 °C. Cathode and anode assemblies are rotated in the

Table 1. Major spent driver fuel composition and available e.m.f. (Ag) at 450 °C

Element	Weight, kg	Wt%	Metal ion	E_m^0, V	Element	Weight, kg	Wt%	Metal ion	E_m^0, V
U	8.0700	80.596	III	-1.496	Si	0.0288	0.288	-	-
Zr*	1.0800	10.805	IV	-1.088	La	0.0284	0.284	III	-2.126
Na	0.2160	2.160	I	-2.500	Pr	0.0269	0.269	-	-
Nd	0.0931	0.930	III	-2.093	Sr	0.0217	0.217	-	-
Cs	0.0773	0.773	-	-	Tc	0.0182	0.182	-	-
Mo	0.0772	0.771	III	+0.119	Sm	0.0177	0.177	-	-
Ce	0.0542	0.542	III	-2.183	Y	0.0126	0.126	III	-2.109
Pu	0.0414	0.413	III	-1.813	Te	0.0112	0.112	-	-
Ru	0.0407	0.407	III	+0.615	Rh	0.0111	0.111	III	+0.526
Ba	0.0330	0.330	-	-	**Total**	9.9595	99.493		

*Zirconium is the most active of the major noble metal compositions in the fuel; here, the term "noble metal" is defined as the metal and metal ion pairs whose e.m.f. are more noble (less negative) than that of the uranium and its trivalent ion while the term "active metal" is defined vice versa.

salt bath providing mixing during the electrorefining process while a stainless steel stirrer is used to continually mix the cadmium. Detailed schematic diagram of the ER and its process are given in Ref. 3.

The major compositions of a typical anode load of two-chopped drive fuel assemblies are given in Table 1. Table 1 includes only fission product species that have weights greater than 0.1 wt% and the electromotive forces (e.m.f.) for several major fuel components, typically metal elements and their most stable ions, in LiCl-KCl eutectic at 450 °C (Refs. 3, 6, 7).

The main purpose of the electrorefining is to separate uranium from the other fuel components. Once the fuel baskets are inserted in the molten salt electrolyte, the bond sodium and active metal fission products chemically react and displace UCl_3 from the molten salt. Uranium in the fuel segment is electrochemically dissolved from the fuel baskets and deposits on the cathode. Zirconium and noble metal fission products are ideally retained in the cladding hulls. The detailed overall process descriptions can be found in Refs. 8, 9, and 10.

III. DATA COLLECTIONS

The ER was operated under a controlled current mode. The cell voltage, current, anode voltage and cathode voltage were recorded and stored in the DASS. The anode voltage for both fuel baskets (Tag names: IEE329B and IEE329D) and the anodic currents (Tag names: IIE329B and IIE329D) were used for this study. Details of these data sets are listed in Table 2. All data sets were saved as the text files with a time step of 20 seconds. The anode and cathode voltages were measured versus a Ag/AgCl reference electrode.

Table 2. Data information

Run No.	Operation Date	Run No.	Operation Date
1	08/19/97[1]	7	02/08/98[2]
2	09/10/97[1]	8	03/29/98[2]
3	10/24/97[3]	9	04/18/98[2]
4	11/22/97[2]	10	05/10/98[1]
5	12/05/97[3]	11	06/04/98[1]
6	01/03/98[3]	12	06/24/98[1]

[1]Data set contains measured values of both fuel baskets.
[2]Data set contains measured values of the fuel basket B only (IEE329B and IIE329B).
[3]Data set contains measured values of the fuel basket D only (IEE329D and IIE329D).

IV. SIGNAL STATISTICAL METHODOLOGY AND PROCEDURES

In general, an anodic process predominantly controlled the overall electrorefining rate. Typical current and anodic voltage curves for different runs, Run No. 3, 10, 11, and 12, are shown in Figures 1A-1D, respectively. It should be noted that the measured values of basket B were used and plotted as examples for Run No. 10, 11, and 12. Each figure shows that the anodic voltage gradually increases, as the uranium is electrochemically dissolved from the anode baskets. In order to retain other fuel components, the current was adjusted and generally reduced while the anode baskets were being depleted. Aside from this observation and similarity, all plots do not constitute the same pattern of operation that will allow a full understanding for signal detection or analysis. That is, these figures: (1) show complex patterns where currents were adjusted and shut-off due to limited

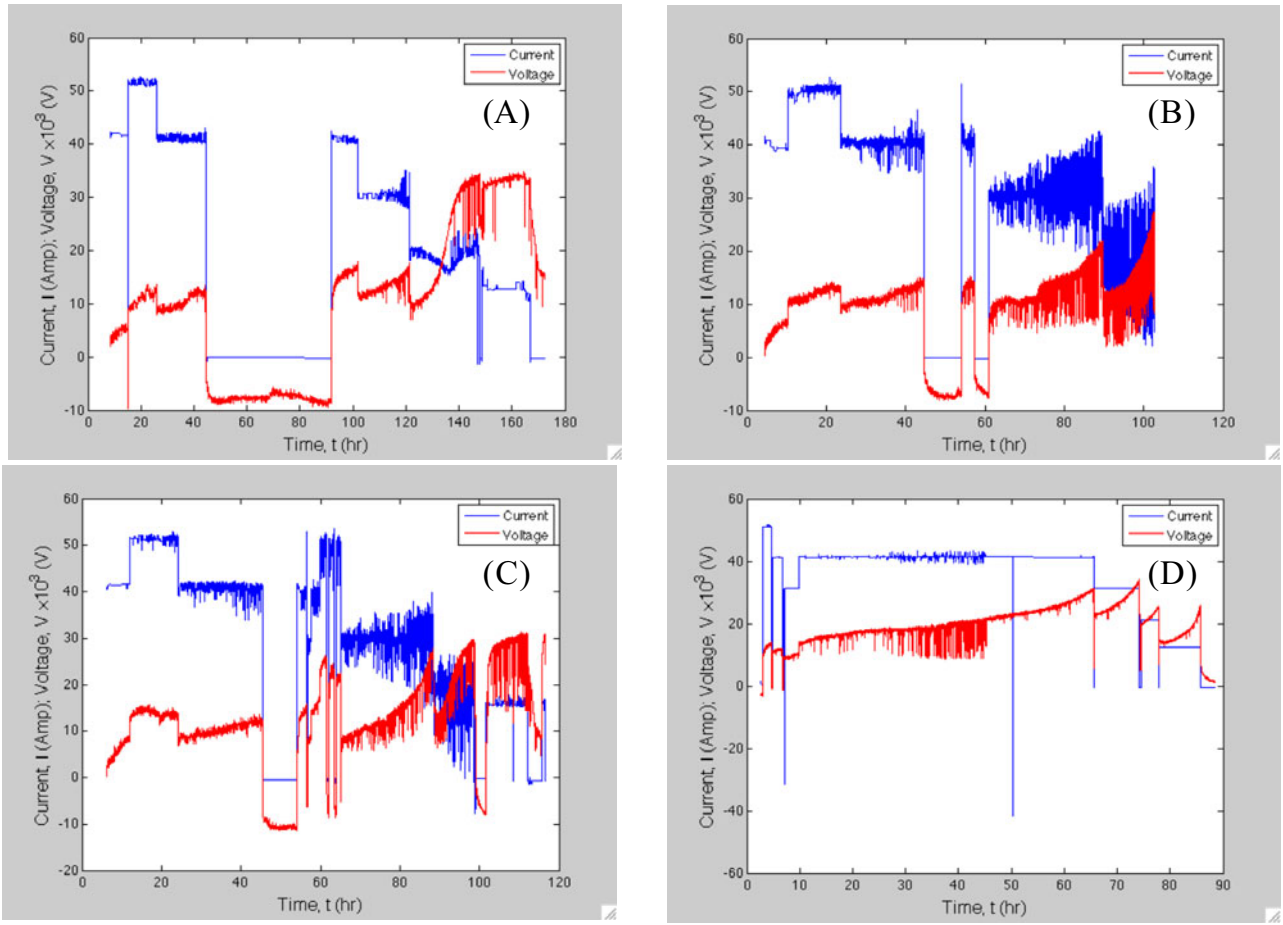

Figure 1. Voltage and current plots of (A) Run No. 3, (B) Run No. 10, (C) Run No. 11, and (D) Run No. 12.

Ampere-hour or cut-off cell voltage, and (2) do not have distinct correlation.

Therefore, a statistical method was applied to find the correlation or pattern among these data sets. All statistical analysis and calculation were performed on a Mac workstation. The numerical scheme was implemented with the commercial software package *Matlab*.

In this first step, a resistance value with respect to the given time, $\Omega(t_i)$, is based on the simple Ohm's Law:

$$\Omega(t_i) = V(t_i)/I(t_i)$$

where $V(t_i)$ and $I(t_i)$ are the voltage and the current with respect to the given time, respectively. Then, the noise signal or infinite outlier at which $I(t_i) = 0$ is being removed to smooth out the data sets. With this first filtering process, the resulting plot can be seen in Figure 2. Run No. 3 is used as an example in this figure. Here, the tolerance value, ε, is given as 0.01 and if $|\Omega(t_i) - \Omega(t_{i+1})| > \varepsilon$, then $\Omega(t_{i+1})$ is set as $\Omega(t_i)$. Figure 2 also shows a gap in the data set that can still be seen in the plot.

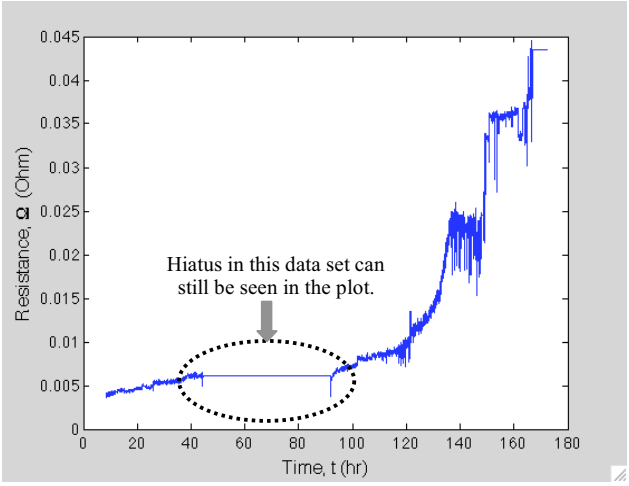

Figure 2. Anodic resistance plot of Run No. 3 after removing noise signal or infinite outlier.

The second part of this method is to obtain a continuous flow pattern plot of $\Omega(t_i)$. In this process, an analogy of Ampere-hr relationship is applied to the above result. An amount of primary product can be formed or transferred based on the proportionality quantity of electricity passed. In this case, an Ampere-hr is simply an area underneath a current plot versus time, that is $I \times t$. Thus, an accumulation of current as the function of time can provide continuous information across the operational domain and can be normalized by the total current summation. Periods providing continuous information can be distinct from a shutoff period or period without any important information.

The third step is to use the screening criterion to obtain the new scale time and to provide new continuous resistance information from the cumulative current information. This information is an observable quantity that may be used to infer kinetic information. This new time frame is based on storing the information based on Ampere-hr basis except removing the outlier or non-useful values in the system. Figures 3 shows the resistance plot after applying the normalized cumulative current technique. A histogram technique is lastly applied to Figure 3 to show a distribution of resistance in that experimental run, as shown in Figure 4.

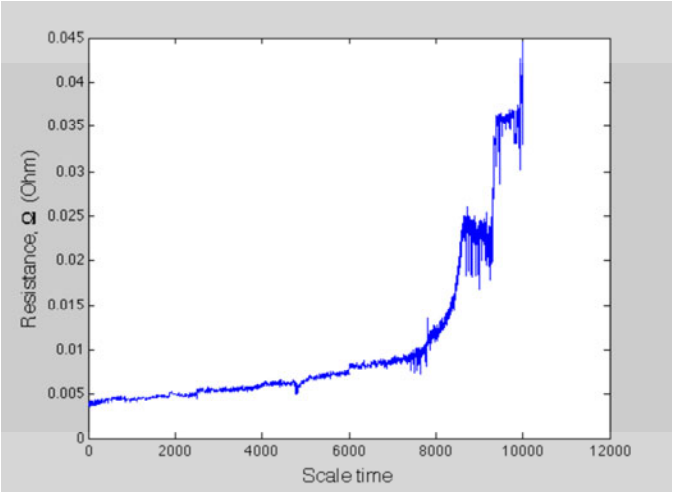

Figure 3. Resistance vs. scale time showing the continuous resistance information of Run No. 3.

V. RESULTS AND DISCUSSION

Figures 5A – 5D show the resistance versus scale time for different experimental runs, Run No. 3, 10, 11, and 12, respectively. Here, the resistance values from the anodic basket for different experiments are in the same range. These curves show the same trend with different fluctuation. The similarity among them can be seen better than the information given in Figures 1A – 1D in comparison. The plots show that in the low resistance range, it requires a relatively small electrical potential difference for electrochemical reaction rates to take place and keep up with the applied current. On the contrary, a large electrical potential difference is required in order to keep the reaction rates in coincide with the applied current, which is corresponding to high resistance range region. These figures show the two regions for the anodic resistance. The first region is the gradual increase area as the electrorefining run progresses; this ranges from 0.001 ohm to about 0.006 ohm. And, the second region is the sharp increase area from 0.006 ohm up to 0.030 ohm. Ref. 3 reports the observation similar to the first region as well. In their work, the anodic resistance increases in the range of 0.003 – 0.007 ohm after passing about 3,000 Ampere-hr. This observation indicates that at least one of the fundamental processes is experiencing a slow down and is being compensated by an increased potential difference between the anode and cathode. The results from these plots confirm the idea of a shrinking core mechanism presented by Ref. 3 at which the anodic resistance increases based on the increase of the electric driving force (Ref. 11). The gradual increase reaches its plateau as the uranium in a fuel segment, viewing as a core, is shrinking as the dissolution reactions progress. The second regions may be used to explain other reactions of fission products during the electrorefining process.

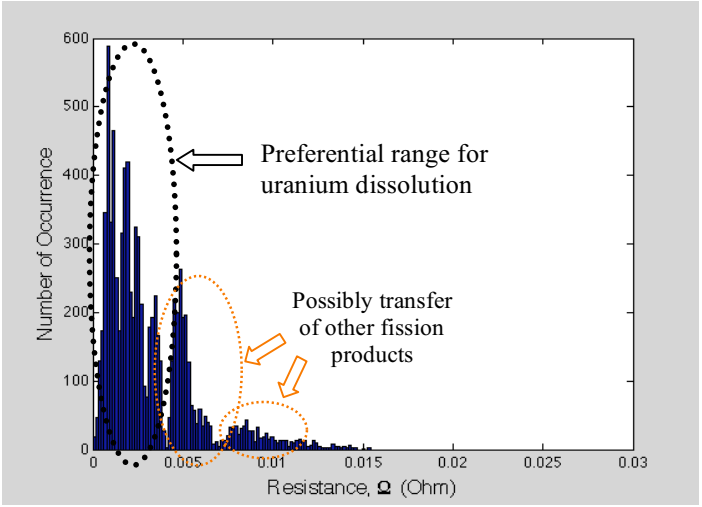

Figure 4. A histogram plot showing number of occurrence for resistance values of Run No. 3 according to the new scale time.

The histograms of number of occurrence (known as *number frequency*) for Figures 5A – 5D are plotted and shown in Figures 6A – 6D, respectively. The results reveal that the peaks in these figures occur around 0.003 ohm. From this observation, the mean resistance value (<Ω>) and its standard deviation of the peak for each run were calculated to help determining the resistance range at which uranium dissolution takes place during the electrorefining process. The calculated results (values are

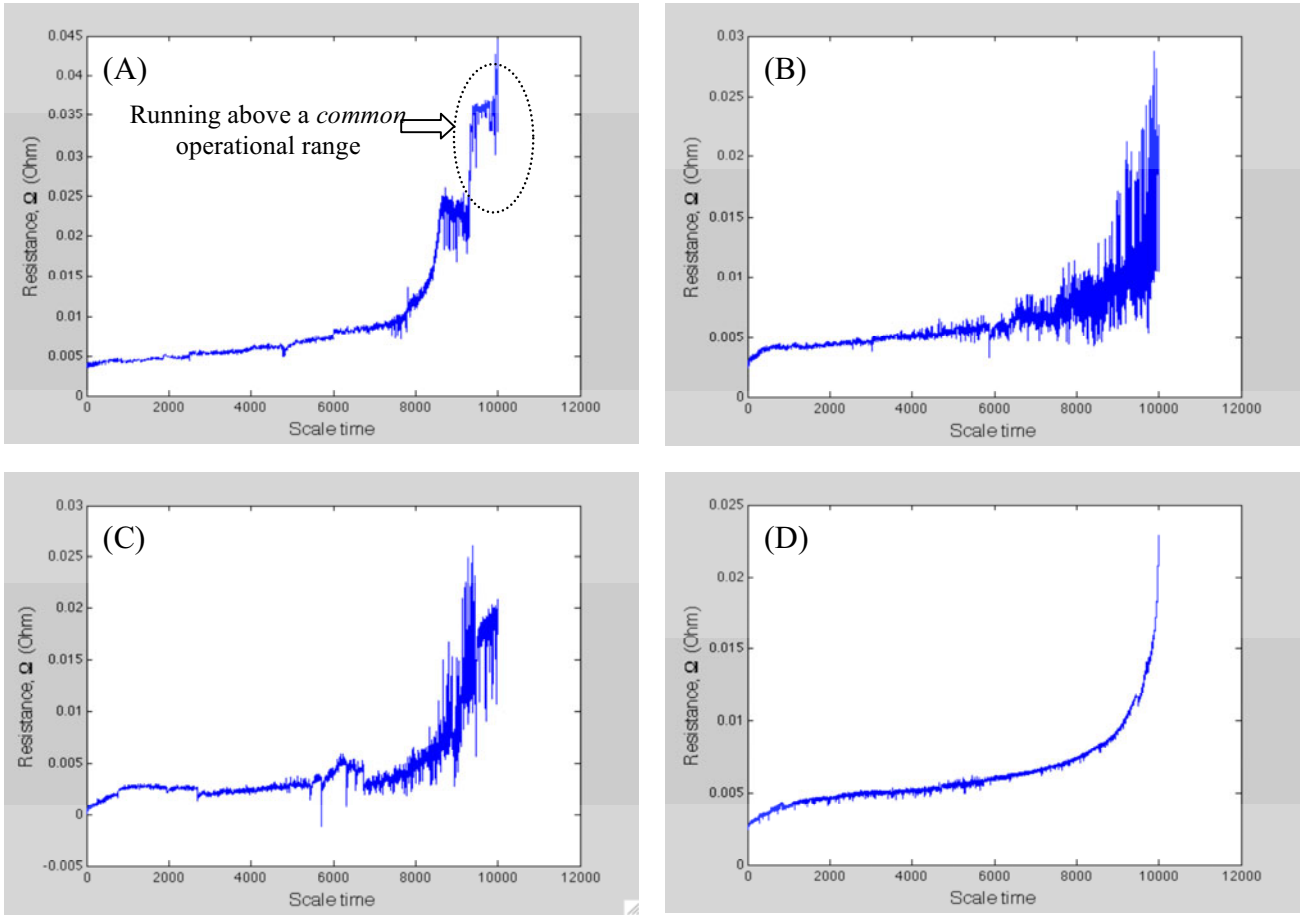

Figure 5. Resistance vs. scale time showing the continuous resistance information of (A) Run No. 3, (B) Run No. 10, (C) Run No. 11, and (D) Run No. 12.

Table 3. Statistical values of anodic resistance for each experimental run

	Anodic basket B		Anodic basket D	
Run No.	**Mean, ohm**	**Standard deviation**	**Mean, ohm**	**Standard deviation**
1	0.001799	0.001244	0.003013	0.001169
2	0.002235	0.000974	0.003961	0.001390
3	-	-	0.003639	0.000836
4	0.002047	0.000574	-	-
5	-	-	0.004559	0.001017
6	-	-	0.002794	0.001147
7	0.002639	0.001147	-	-
8	0.002724	0.000874	0.003115	0.000832
9	0.002555	0.001224	-	-
10	0.002359	0.001255	0.002574	0.001364
11	0.002794	0.001183	0.002765	0.001304
12	0.003411	0.000904	0.002423	0.001128
Overall[1]	0.002856 ± 0.000904	0.000685 ± 0.000217		

[1] Results are accounted for both anodic baskets.

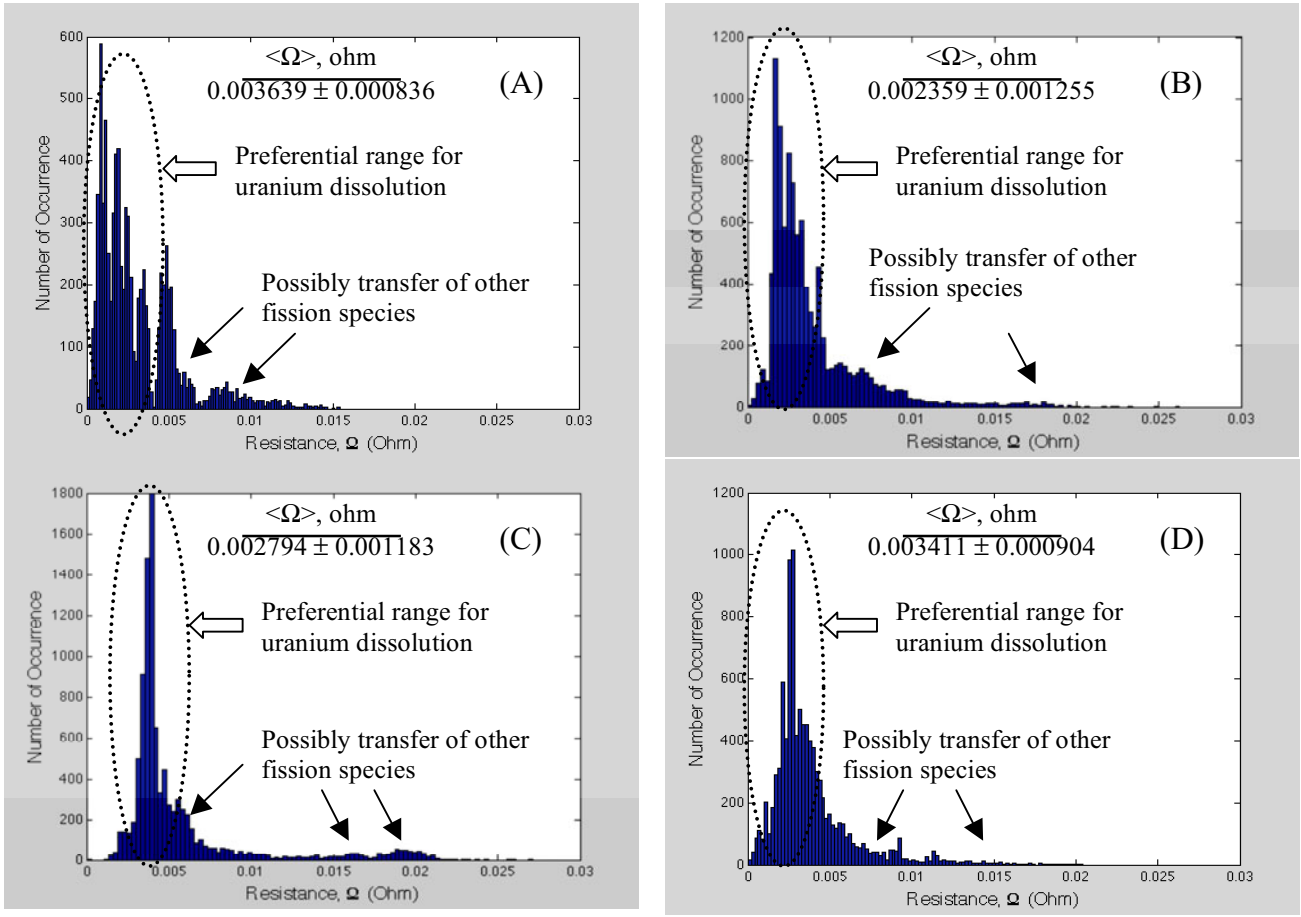

Figure 6. A histogram plot showing number of occurrence for anodic resistance values of (A) Run No. 3, (B) Run No. 10, (C) Run No. 11, and (D) Run No. 12.

based on $\Omega < 0.007$) are listed in Table 3. Since the main goal of using the ER is to electrotransport uranium from fuel elements to refined deposits, these results suggest that mostly uranium would be preferentially transferred around 0.00217 - 0.00354 ohm. This range confirms the observation reported by Ref. 3 for their Mk-IV analysis on the resistance range for uranium dissolution experiments. Figures 6A – 6D show that there are other minor peaks that give trends of possible transfer of other fission products. It is possible that there are co-dissolutions of zirconium as well for the second main peak as noble metals since zirconium is the most active of the major noble metal compositions in the fuel. Understanding the correct behaviors and characteristics of these peaks with respect to uranium dissolution is currently being studied.

VI. SUMMARY

A new statistical invariance technique has been proposed to help predict and yield important information and characteristics of the electrorefining process of spent driver fuel in a molten LiCl-KCl-UCl_3 system. The voltage and current data from the experiments conducted during 1997 and 1998 time-frame present a challenging time-series analysis problem. The results obtained with the developed methodology reveal interesting outcomes, showing that there is a resemblance among these data sets. Based on adjusted resistance curves and through histogram analysis, the outcomes reveal that the uranium dissolution occurs at the resistance of approximately 0.003 ohm. This observation is strikingly similar to that reported by other investigators (Ref. 3). It is suspected that transfer of other fission products may possibly represent other peaks in the distribution. It is hoped that this new analysis will contribute to significant improvement in the design of ER process by detecting the uranium dissolution through its resistance characteristic distribution across the system.

REFERENCES

1. T. Kobayashi, R. Fujita, M. Fujie, and T. Koyama, Polarization effects in the molten salt electrorefining of spent nuclear fuel," *Journal of*

Nuclear Science and Technology, **32**(7), 653 (1995).
2. R.W. Benedict and H.F. McFarline, "EBR-II spent fuel treatment demonstration project status," *Radwaste Magazine,* July, 23-25 (1998).
3. S. X. Li, and M. F. Simpson, "Anodic process of electrorefining spent driver fuel in molten LiCl-KCl-UCl_3/Cd system," *Minerals & Metallurgical Processing*, **22**(4), 192 (2005).
4. R. K. Ahluwalia, T. Q. Hua, "Electrotransport of uranium from a liquid cadmium anode to a solid cathode," *Nuclear Technology*, **140**(1), 41 (2002).
5. R. K. Ahluwalia, T. Q. Hua, and V. DeeEarl, "Uranium transport in a high-throughput electrorefiner for EBR-II blanket fuel," *Nuclear Technology*, **145**(1), 67 (2004).
6. Bard, A. J., *Encyclopedia of Electrochemistry of the Elements*, *Vol. X., Fused Salt Systems*, p. 68, Marcel Dekker, Inc., New York (1976).
7. J. A. Plambeck, "Electromotive force series in molten salts," *Journal of Chemical and Engineering Data*, **12**(1), 77 (1967).
8. J. P. Ackerman, "Chemical basis for pyrochemical reprocessing of nuclear fuel," *Industrial & Engineering Chemistry Research*, **30**(1), 141 (1991).
9. Y. I. Chang, "The integral fast-reactor," *Nuclear Technology*, **88**(2), 129 (1989).
10. R. D. Mariani, *Basics of electrorefining in the fuel cycle facility* in IFR Technical Memorandum, No. 212, pp. 1-21 (1993).
11. O. Levenspiel, *Chemical Reaction Engineering, 2nd Ed.*, pp. 360-368, John Wiley and Sons, Inc., Boston (1972).